ResearchGate

See discussions, stats, and author profiles for this publication at: https://www.researchgate.net/publication/231408533

Free jet-cooled laser-induced fluorescence spectrum of methoxy. 1. Vibronic analysis of the ~A and ~X states

ARTICLE *in* THE JOURNAL OF PHYSICAL CHEMISTRY · OCTOBER 1988

Impact Factor: 2.78 · DOI: 10.1021/j100332a014

CITATIONS
56

READS
26

6 AUTHORS, INCLUDING:

Stephen Foster
Mississippi State University
51 PUBLICATIONS **1,071** CITATIONS
SEE PROFILE

Prabhakar Misra
Howard University
90 PUBLICATIONS **369** CITATIONS
SEE PROFILE

Terry A Miller
The Ohio State University
436 PUBLICATIONS **7,256** CITATIONS
SEE PROFILE

Available from: Prabhakar Misra
Retrieved on: 02 February 2016

Free Jet Cooled Laser-Induced Fluorescence Spectrum of Methoxy. 1. Vibronic Analysis of the $\tilde{A}$ and $\tilde{X}$ States

Stephen C. Foster,† Prabhakar Misra, Tai-Yuan D. Lin, Cristino P. Damo, Christopher C. Carter, and Terry A. Miller*

Laser Spectroscopy Facility, Department of Chemistry, The Ohio State University, 120 West 18th Avenue, Columbus, Ohio 43210 *(Received: February 8, 1988)*

The methoxy free radical has been formed in a supersonic free jet expansion by KrF photolysis of methyl nitrite. Its laser-induced fluorescence excitation and wavelength-resolved emission spectra have been recorded at low temperature. This paper reports the vibronic analysis of the CH_3O and CD_3O $\tilde{A}^2A_1 \leftrightarrow \tilde{X}^2E$ electronic spectra. A new value for the electronic origin has been determined as well as a nearly complete set of vibrational frequencies.

I. Introduction

The methoxy radical is one of the most interesting and most widely studied[1-10] of all organic free radicals. Much of the interest in CH_3O lies in its ubiquity. The radical is well-known to play important roles in combustion and atmospheric pollution chemistry. It is also of considerable interest in astrophysical work. Since CH_3O is indeed a very reactive free radical, highly sensitive, unambiguous diagnostic techniques for CH_3O are quite valuable. Almost exclusively, these diagnostic techniques are spectroscopic, most usually based upon the $\tilde{A}^2A_1 \leftrightarrow \tilde{X}^2E$ optical transition in the near-ultraviolet, analogous to the $A^2\Sigma \leftrightarrow X^2\Pi$ transition in the closely related, but nonorganic, free radical OH. This latter transition is usually described in "one-electron parlance" as corresponding to the promotion of a p-σ bonding electron to fill the nearly nonbonding p-π orbitals mainly localized on the O atom, with an analogous explanation being appropriate for CH_3O.

However, diagnostic considerations are not the only ones which make spectroscopic studies of methoxy interesting. Theoretical questions about both the ground ^2E and excited $^2A_1$ states are extensive. Indeed, since methoxy is one of the simplest of polyatomic free radicals, it has been the subject of several ab initio calculations[11-15] which are by no means in complete agreement with respect to many of its properties.

Methoxy is also of particular theoretical significance from another point of view. It has nominal C_{3v} symmetry, but its ground electronic state is doubly degenerate and subject to a Jahn-Teller distortion. Such a distortion should produce a very unique and interesting spectrum, particularly considering methoxy's moderate spin-orbit splitting ($\sim$60 cm^{-1}). Consequently, methoxy's spectrum should give us the best means for understanding any Jahn-Teller distortion and its interaction with the spin-orbit coupling.

As mentioned above, the literature on methoxy is by most measures vast. Particularly germane to this work, there recently have been a microwave study,[3] a laser-induced fluorescence (LIF) study,[9] and a "cold" jet emission study.[10] Although we have been involved[16] in a series of supersonic free jet LIF studies of larger alkoxy radicals, e.g., C_2H_3O, C_2H_5O, and C_3H_7O, we initially believed that the spectroscopy of methoxy was generally well understood and required little further investigation.

On closer inspection, however, we recognized that, despite the extensive spectroscopic investigations of the radical, none of the bands of the well-known $\tilde{A}^2A_1 \leftrightarrow \tilde{X}^2E$ UV transition has ever been subjected to a detailed rotational analysis (however, note the pioneering work of Powers et al.[7]), resulting, of course, in a lack of knowledge about the excited-state "rotational" parameters. We also realized that the analysis of the relatively simple, cold jet LIF rotational spectra, along with the existence of ground-state parameters from the microwave work, should yield excellent excited-state molecular parameters.

† Present address: Department of Chemistry, Florida State University, Tallahassee, FL 32306.

TABLE I: CH_3O $\tilde{A}^2A_1$-$\tilde{X}^2E_{3/2}$ Origin Frequency (cm^{-1})

<1975	1975-1980	1980-1985	>1985
30 465[a]	32 800[b]	31 536[d]	31 690[h,f]
	31 538[c]	31 540[e,f]	32 306[i,f]
		31 530[g]	31 644.5[j,f]

[a] Reference 1. [b] Reference 4. [c] Reference 5. [d] Reference 6. [e] Reference 7. [f] Value quoted specifically for $^2E_{3/2}$ state; other references do not distinguish between $^2E_{3/2}$ and $^2E_{1/2}$ states. [g] Reference 8. [h] Reference 9. [i] Reference 10. [j] This work and ref 17. The value quoted is measured from the lowest $\tilde{X}^2E_{3/2}$ rotational level, $K = 0$, $J = 0.5$, to the lowest $\tilde{A}^2A_1$ rotational level, $N = 0$, $K = 0$.

Once this work began, we discovered that there were a large number of other spectroscopic questions concerning methoxy that are not properly resolved. For instance, Table I summarizes nine different reports purporting to give frequencies for the origin of the methoxy UV electronic transition. Clearly, one must know which band to analyze as the origin to obtain "r_0 rotational" parameters.

We have thus carried out a detailed study of the vibronic spectrum of methoxy as a necessary prelude to the rotational analysis of its bands. The results of this analysis, which are described in this paper, yield a new and, we believe, reliable value for the electronic origin as well as a nearly complete set of vibrational frequencies for both the $\tilde{X}$ and $\tilde{A}$ states. These frequencies are significantly revised from earlier reports. Figure 1 shows a schematic representation of these vibrational motions. A following paper[17] describes the rovibronic analysis of the 0_0^0 and

(1) Style, D. W. G.; Ward, J. C. *Trans. Faraday Soc.* **1953**, *49*, 999.
(2) Radford, H. E.; Russell, D. K. *J. Chem. Phys.* **1977**, *66*, 2222. Russell, D. K.; Radford, H. E. *J. Chem. Phys.* **1980**, *72*, 2750.
(3) Endo, Y.; Saito, S.; Hirota, E. *J. Chem. Phys.* **1984**, *81*, 122.
(4) Ohbayashi, R.; Akimoto, H.; Tanaka, I. *J. Phys. Chem.* **1977**, *81*, 798.
(5) Wendt, H. R.; Hunziker, H. E. *J. Chem. Phys.* **1979**, *71*, 5202.
(6) Inoue, G.; Akimoto, H.; Okuda, M. *J. Chem. Phys.* **1980**, *72*, 1769.
(7) Powers, D. E.; Hopkins, J. B.; Smalley, R. E. *J. Phys. Chem.* **1981**, *85*, 2711.
(8) Ebata, T.; Yanagishita, H.; Obi, K.; Tanaka, I. *Chem. Phys.* **1982**, *69*, 27.
(9) Fuke, K.; Ozawa, K.; Kaya, K. *Chem. Phys. Lett.* **1986**, *126*, 119.
(10) Brossard, S. D.; Carrick, P. G.; Chappell, E. L.; Hulegaard, S. C.; Engelking, P. C. *J. Chem. Phys.* **1986**, *84*, 2459. See also the even more extensive list of references in this paper.
(11) Yarkony, D. R.; Schaefer, H. F., III; Rothenberg, S. *J. Am. Chem. Soc.* **1974**, *96*, 656.
(12) Ohkubo, K.; Fujita, T.; Sato, H. *J. Mol. Struct.* **1977**, *36*, 101.
(13) Bent, G. D.; Adams, G. F.; Bartram, R. H.; Purvis, G. D.; Bartlett, R. J. *J. Chem. Phys.* **1982**, *76*, 4144.
(14) Jackels, C. F. *J. Chem. Phys.* **1982**, *76*, 505.
(15) Saebø, S.; Radom, L.; Schaefer, H. F., III *J. Chem. Phys.* **1983**, *78*, 845.
(16) Foster, S. C.; Hsu, Y.-C.; Damo, C. P.; Liu, X.; Kung, C.-Y.; Miller, T. A. *J. Phys. Chem.* **1986**, *90*, 6766.

0022-3654/88/2092-5914$01.50/0 © 1988 American Chemical Society

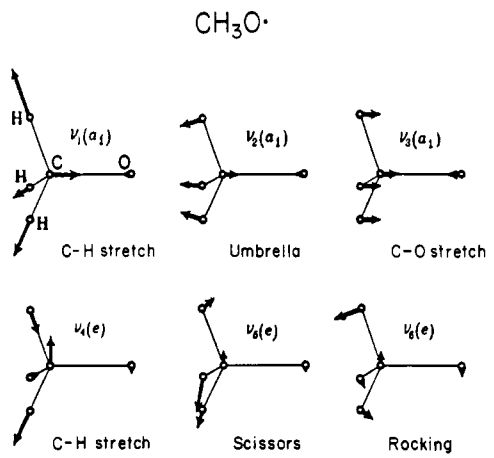

Figure 1. Schematic representations of the three a_1 and three doubly degenerate e vibrations of methoxy.

3_0^1 bands of CH_3O which yield the first rotational parameters for the $\tilde{A}$ state and, perhaps surprisingly, slightly revised values for the $\tilde{X}$ state. A complete vibrational analysis of the ground state requires an unraveling of the Jahn–Teller effect therein. That Jahn–Teller analysis is deferred to a subsequent paper.

The vibronic analysis of this paper is based upon two kinds of data taken in a supersonic free jet expansion wherein very cold methoxy radicals with rotational temperatures in the range 3–25 K are observed. Laser excitation of these cold radicals are recorded, without rotational resolution, to give an overview of the vibronic structure of the excited state. Once over 6500 cm^{-1} of this spectrum has been recorded, individual bands can be laser excited and the resulting emission wavelength-resolved with a monochromator and optical multichannel analyzer. These results are used to determine the vibronic structure of the ground state and elucidate ambiguous excited-state vibronic assignments. Experiments have been performed on both CH_3O and its perdeuterio analogue, CD_3O.

II. Experimental Section

The methoxy and perdeuteriated methoxy radicals were formed in the excimer laser photolysis of their respective precursors, the alkyl nitrites (CH_3ONO and CD_3ONO) seeded in low concentration into a supersonic free jet expansion. The radicals were then excited by a probe dye laser, and fluorescence was collected with an $f/1$ lens. Fluorescence excitation spectra were recorded by scanning the excitation wavelength and monitoring total fluorescence. Dispersed fluorescence spectra were obtained by exciting the radicals at the wavelength of a rotational line near the band maxima. After passing through a monochromator at a fixed grating position, the fluorescence was then focused onto the diode array detector of an optical multichannel analyzer (OMA).

The nitrites were synthesized by the dropwise addition of dilute sulfuric acid to a solution of sodium nitrite and the corresponding alcohol.[18] Gaseous at room temperature, the nitrites were collected at −78 °C with an acetone/dry ice bath. FT-IR spectra (Mattson Instruments CYGNUS 25) of the gas showed infrared bands highly characteristic of alkyl nitrites[19] and the absence of any significant impurities.

Our experiments coupling supersonic free jet expansions with laser-induced fluorescence have been previously described.[16] Briefly, the precursor was seeded in a He carrier gas at ~10 atm and introduced into the chamber through a commercial pulsed nozzle (Newport BV-100) with a 0.5-mm orifice. A KrF (248 nm) excimer laser (Lumonics Excimer-510) beam crossed the expansion within 2 mm of the nozzle exit to photolyze the RO–NO bond. The probe laser was the frequency-doubled output of a XeCl (308 nm) excimer-pumped dye laser (Lumonics Excimer-510 and HyperDye-300). The dye laser fundamental (Exciton dyes: C540A, Rh590, KR620, Rh640, SR640, and DCM) was doubled by an autotracking second-harmonic generator with a KDP crystal (INRAD Autotracker II). This UV probe laser beam then excited the radicals ~6 mm further downstream from the photolysis laser, and fluorescence was collected through a quartz lens at right angles to the plane of the counterpropagating laser beams and the nozzle.

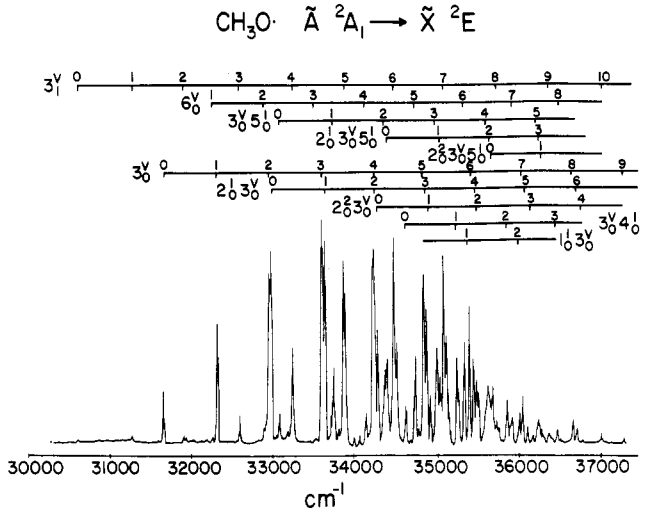

Figure 2. Laser excitation spectrum of CH_3O. The vibrational assignments are indicated above. Only one hot-band sequence, 3_1^v, could be detected and it only weakly, indicating that the radical is relatively cold vibrationally as well as rotationally.

On one side of the plane, the excitation spectra were obtained. Total fluorescence detected by a photomultiplier tube (EMI 9659A) was input to a custom-built gated integrator with a gate width set at 3.6 μs. The integrated output was then digitized by a 12-bit analog-to-digital converter (Tecmar Lab Master), averaged, and stored in a microcomputer (IBM PC/XT) for further processing. The Lab Master also provided the interface between the microcomputer and the dye laser, thereby permitting scanning of the excitation wavelength. All excitation spectra were calibrated by reference to the iodine frequency standard.[20]

On the other side of the chamber, total fluorescence was focused onto the entrance slit (0.150 to 1.000 mm) of a 1/3-m monochromator (Instruments SA HR-320). At the exit plane was a 1024-element diode array detector cooled to −25 °C. Data were collected with the detector in the pulsed mode, which allowed the scattered light to be temporarily rejected and resulted in the correct relative intensities between the fluorescence resonant with the exciting wavelength and the rest of the spectra. After 10 min of integration, the signal from the detector was processed by the OMA (EG&G PARC Model 1460) and provided wavelength-resolved emission spectra. Stored data were then transferred to the microcomputer for further analyses. Dispersed fluorescence spectra were calibrated with the iron/neon lines of the iron hollow-cathode spectrum.[21]

III. Results: Methoxy, CH_3O

A. The Electronic Origin. The excitation spectrum, shown in Figure 2, is dominated by a long progression of bands which starts at approximately 31 650 cm^{-1} and is spaced by 660 cm^{-1}. Dispersed fluorescence spectra of the 31 650-cm^{-1} band, discussed in detail later, clearly show that this feature does not originate from a hot ground-state level, whereas all the features to the red of this band are seen to be hot. This feature is therefore assigned as the $\tilde{A}^2A_1 \leftrightarrow \tilde{X}^2E_{3/2}$ component of the 0_0^0 band. No excitation

(17) Liu, X.; Damo, C. P.; Lin, T.-Y.; Misra, P.; Foster, S. C.; Yu, L.; Miller, T. A. *J. Phys. Chem.*, in press.
(18) Blatt, A. H., Ed. *Organic Syntheses*, Collective Volume 2; Wiley: New York, 1943; p 363.
(19) (a) Pouchert, C. J., Ed. *The Aldrich Library of Infrared Spectra*, 3rd ed.; Aldrich Chemical Co.: Milwaukee, 1981. (b) Rook, F. L.; Jacox, M. E. *J. Mol. Spectrosc.* **1982**, *93*, 101.
(20) Gerstenkorn, S.; Luc, P. *Atlas du Spectre d'absorption de la Molécule d'Iode*; Centre National de la Recherche Scientifique: Paris, 1978.
(21) Crosswhite, H. M. *J. Res. Natl. Bur. Stand. Sect. A* **1975**, *79A*, 17.

spectrum is observed from the higher lying $\tilde{X}^2E_{1/2}$ spin–orbit component, presumably because of its essentially nonexistent population at the very low temperature of the jet expansion. Small differences quoted in band positions between the analyses in this paper and ref 17 reflect the error introduced by using band maxima (quoted throughout this paper) rather than the true band origins (used in ref 17).

Traditionally, the origin of a spin–orbit split transition is taken as the mean of the $^2E_{3/2}$ and $^2E_{1/2}$ state's excitation frequencies. Since the ground-state spin–orbit splitting is 63 cm^{-1}, this places the traditionally defined origin at 31 618 cm^{-1}, using band maxima. The detailed[17] rotational analysis of this band gives a more accurate value of 31 614.5 cm^{-1} for the origin and 62.0 cm^{-1} for the spin–orbit splitting. The value of 31 644.5 cm^{-1} quoted in Table I is the frequency of the transition from the lowest rotational level of the $^2E_{3/2}$ state, a value more comparable to the other entries in Table I.

It should be noted here that there has been a good deal of controversy (see Table I) about the assignment of the methoxy origin band and that we present another new value. Most earlier work involved hot spectra,[1,4,5,6] which are much more difficult to interpret unambiguously. Three other jet-cooled spectra have been published which might have been expected to produce a single consistent value for the origin. In 1981 Powers et al.[7] recorded the first cold spectrum of methoxy. They show a portion of their spectrum between 31 440 and 31 690 cm^{-1}, with the origin centered at 31 540 cm^{-1} in their Figure 2. We have carefully checked the calibration of our present spectrum and can only conclude that there must be a calibration error in ref 7.

Brossard et al.[10] made an extensive study of the emission from a jet-cooled corona discharge and proposed a value of 32 306 cm^{-1} for the $^2E_{3/2}$ subband of the origin. Although somewhat rotationally cooled, the spectrum was characteristic of a vibrationally very hot $\tilde{A}$ state and contained a large number of bands. Their origin is in good agreement with our 3_0^1 band. It appears that these authors simply missed the first member of the ν_3' progression.

Another recent study, published by Fuke et al.,[9] is very similar to the spectrum presented here. It was surprising that their reported origin, 31 690 cm^{-1}, differs from the value given here. A careful inspection of Fuke et al.'s Figure 1 reveals that all features below 32 000 cm^{-1} differ by 40 cm^{-1} from our values, whereas both studies are in good agreement above 32 000 cm^{-1}. As noted above, our calibration has been carefully examined and we must conclude that a calibration error was also made in ref 9.

B. $\tilde{A}^2A_1$ Vibrational Assignment. Although the spectrum shown in Figure 2 is rotationally and vibrationally cold, it is quite complex, containing a large number of vibrational bands. The complexity reflects the fact that all six fundamental vibrational modes (see Figure 1) of methoxy are observed—not just the three totally symmetric vibrations. The three e vibrations gain intensity in excitation because of the Jahn–Teller distortion of the ground electronic state.[22] One might consider that the eigenfunction which describes the vibrationless level of the ground electronic state is mixed with the e vibration eigenfunctions of the ground state by the Jahn–Teller effect. Since the vibrationless level has partial e character, transitions to levels with e vibronic symmetry in the excited electronic state become allowed.

Most of the bands observed in the excitation spectrum can be seen to lie in progressions with a 660-cm^{-1} vibrational interval. Ab initio calculations predict[11] a large change in the C–O bond length between the $\tilde{A}$ and $\tilde{X}$ states, and consequently we expect a long progression in ν_3', the CO stretching vibration. This large change in the CO bond length has now been confirmed[17] by the rotational analysis of the 0_0^0 band. It seems clear that the 660-cm^{-1} interval corresponds to ν_3', as noted by several earlier authors.[6,9,10]

TABLE II: Observed Vibrational Intervals (in cm^{-1}) for Several CH_3X Molecules

mode	$\tilde{X}$ CH_3F[a]	$\tilde{X}$ CH_3Cl[a]	$\tilde{X}$ CH_3F^+[b,c]	$\tilde{X}$ CH_3O[d]	$\tilde{A}$ CH_3O[d]
ν_1	2965	2966		2840	3079
ν_2	1475	1355	1314	1362	1315
ν_3	1048	732	938	1047	660
ν_4	2982	3042		2774(?)	2962
ν_5	1471	1455		1487	1407
ν_6	1196	1015	694	653	595

[a] Reference 23. [b] References 24 and 25. [c] The two higher frequency vibrations observed by ref 24 and 25 are assigned in agreement with ref 24. The 694-cm^{-1} vibration, only observed by ref 25, is reassigned as ν_6. [d] Present work.

A closer inspection of the ν_3' progression reveals that the 3_0^2 and 3_0^3 bands are doubled and that the 3_0^{2x-2} and 3_0^{2x-1} ($x \geq 1$) bands, in general, form multiplets with x members. This multiplet structure, noted by earlier authors,[6,9,10] arises because of an accidental near degeneracy of ν_2' and $2\nu_3'$. As a result of the Fermi resonance, ν_2' gains intensity from $2\nu_3'$. Dispersed fluorescence spectra of the first diad show that the lower frequency band is predominantly 3_0^2, whereas the higher frequency feature is best identified as 2_0^1. This analysis of ν_3 and ν_2 is consistent with most of the earlier work, but differs from that of Brossard et al.[10] because of their error in assigning the electronic origin and because they have reversed the assignment of ν_2' and ν_3'. It can also be noted that the 632-cm^{-1} value for ν_2' given by Brossard et al.[10] is very low for this type of umbrella motion and inconsistent with the corresponding vibrations of the methyl halides (see Table II); the C–O geometry change is unlikely to substantially effect this frequency.

Several other obvious progressions in ν_3' can be seen in Figure 2, with first members at 33 057 cm^{-1} (1407 cm^{-1} from the origin), 34 375 cm^{-1} (2725 cm^{-1}), 34 612 cm^{-1} (2962 cm^{-1}), and 35 389 cm^{-1} (3739 cm^{-1}). The dispersed fluorescence studies, to be discussed later, show that the 1407, 2725, and 2962-cm^{-1} progressions can be assigned to bands with e vibrational character. In contrast, the 3739-cm^{-1} band is characteristic of an a_1 vibrational mode. Since this latter band is not an overtone or combination band of ν_2' or ν_3', it might be assigned as ν_1'. However, 3739 cm^{-1} appears to be too large when compared to typical methyl halide stretching frequencies, as shown in Table II. It is more likely that the band is $1_0^1 3_0^1$ and that 1_0^1 is too weak to be observed. This assignment reduces ν_1' to 3079 cm^{-1}. A band is observed 3076 cm^{-1} from the origin, but it is anomalously intense for 1_0^1. Furthermore, it shows a completely different ground-state vibrational structure from the 3739-cm^{-1} band when pumped and dispersed. A probable assignment for this 3076-cm^{-1} band, discussed below, is 6_0^5.

The 1407- and 2725-cm^{-1} bands are both e vibrations and differ by the value of ν_2'. They are assigned as 5_0^1 and $2_0^1 5_0^1$. The value adopted for ν_5' is in good agreement with the values seen for methyl chloride and methyl fluoride.

The remaining ν_3' progression, starting 2962 cm^{-1} from the origin, is assigned as 4_0^1 and its combinations with ν_3'. This asymmetric H-stretching frequency is consistent in magnitude with the methyl halide values (see Table II).

One further series of bands can be identified in the excitation spectrum. The first member is seen as a weak shoulder 65 cm^{-1} to the low-frequency side of 3_0^1. The 65-cm^{-1} interval is very close to the ground-state spin–orbit splitting, but the higher members of the progression grow in intensity relative to, and move away from, the members of the ν_3' progression. The 595-cm^{-1} separation of the first members of the progression from the origin, although small, is most likely to be ν_6'. The corresponding methyl fluoride vibration is much larger, but this 595-cm^{-1} value is consistent with the isoelectronic methyl fluoride ion and with the value of ν_6'' observed in the dispersed fluorescence spectra. The progression is thus assigned as 6_0^1, 6_0^2, ... 6_0^8. The lowest members of the

(22) See, for example, the discussion in the chapter by T. A. Miller and V. E. Bondybey in *Molecular Ions: Spectroscopy, Structure, and Chemistry*; Miller, T. A., Bondybey, V. E., Eds.; North-Holland: Amsterdam, 1983; p 201.

(23) Herzberg, G. *Molecular Spectra and Molecular Structure II: Infrared and Raman Spectra of Polyatomic Molecules*; Van Nostrand Reinhold: New York, 1945; p 315.

(24) Stokes, S.; Duncan, A. B. F. *J. Am. Chem. Soc.* **1958**, *80*, 6177.

(25) Karlsson, L.; Jadrny, R.; Mattsson, L.; Chau, F. T.; Siegbahn, K. *Phys. Script.* **1977**, *16*, 225.

TABLE III: CH_3O $\tilde{A}^2A_1 \leftarrow \tilde{X}^2E$ Excitation Spectrum (cm^{-1})

wave-number	rel wavenumber	assignt	wave-number	rel wavenumber	assignt
30606	−1044	3_0^0	35028	3378	$2_0^1 3_0^1 5_0^1$
31265	−385	3_0^1	35077	3427	3_0^7
31650	0	0_0^0	35243	3593	$3_0^1 4_0^1$
31888	238	3_0^2	35327	3677	6_0^6
31917	267	$2_0^1 3_0^0$	35389	3739	$1_0^1 3_0^1$
32245	595	6_0^1	35441	3791	3_0^8
32310	660	3_0^1	35477	3827	$2_0^1 3_0^4$
32576	926	3_0^3	35502	3852	$2_0^2 3_0^2$
32873	1223	6_0^2	35611	3961	$3_0^4 5_0^1$
32937	1287	3_0^2	35634	3984	$2_0^1 3_0^2 5_0^1$
32965	1315	2_0^1	35673	4023	$2_0^2 5_0^1$
33057	1407	5_0^1	35727	4077	3_1^8
33220	1570	3_1^4	35760	4110	
33503	1853	6_0^3	35855	4205	$3_0^2 4_0^1$
33582	1932	3_0^3	35918	4268	6_0^7
33619	1969	$2_0^1 3_0^1$	36010	4360	$1_0^1 3_0^2$
33717	2067	$3_0^1 5_0^1$	36047	4397	3_0^7
33852	2202	3_1^5	36106	4456	$2_0^1 3_0^5$
33968	2318		36168	4518	$2_0^2 3_0^3$
34042	2392		36237	4587	$3_0^5 5_0^1$
34119	2469	6_0^4	36281	4631	$2_0^1 3_0^3 5_0^1$
34209	2559	3_0^4	36303	4653	$2_0^2 3_0^1 5_0^1$
34220	2570	$2_0^1 3_0^2$	36363	4713	3_1^9
34265	2615	2_0^2	36464	4814	$3_0^3 4_0^1$
34350	2700	$3_0^5 5_0^1$	36509	4859	6_0^8
34375	2725	$2_0^1 5_0^1$	36656	5006	3_0^8
34463	2813	3_1^6	36703	5053	$2_0^1 3_0^6$
34612	2962	4_0^1	36773	5123	$2_0^2 3_0^4$
34726	3076	6_0^5	36867	5217	$3_0^6 5_0^1$
34830	3180	3_0^5	36913	5263	$2_0^1 3_0^4 5_0^1$
34864	3214	$2_0^1 3_0^3$	36989	5339	3_1^{10}
34906	3256	$2_0^2 3_0^1$	37272	5622	3_0^9
34991	3341	$3_0^5 5_0^1$			

progression were too weak to pump and observe dispersed fluorescence, but the higher frequency bands 6_0^5 and 6_0^6 showed structure characteristic of e vibronic levels.

Table III lists the observed vibrational band maxima and vibrational assignments. The $\tilde{A}^2A_1$ fundamental vibrational frequencies discussed above are summarized in Table II.

C. $\tilde{X}^2E_i$ Vibrational Assignment. Single vibronic level (SVL) dispersed fluorescence spectra greatly simplify the task of analyzing the ground-state vibrational structure. Much of the congestion, and hence confusion, is removed when all the emission originates from a single rovibronic level.

The dispersed fluorescence spectra observed here can be broadly divided into two general classes: (i) simple, showing strong doubled progressions in the totally symmetric modes (the doubling being spin–orbit splitting) and single lines corresponding to Jahn–Teller active e vibrations; (ii) very complex, containing large numbers of vibrational bands which cannot be explained by six vibrational modes, their harmonic or near-harmonic combinations, and overtones, with their expected degeneracies.

The first class of spectra arise when totally symmetric modes are pumped, a typical example being the 3_0^1 band shown in Figure 3. The second case arises when the degenerate e vibrations of the excited state are pumped, as typified by Figure 4, which shows the 6_0^5 band. Both types of spectra are a consequence of the Jahn–Teller effect.[22] That any of the e vibrations are observed in emission from a totally symmetric mode proves that methoxy has a Jahn–Teller distorted ground state. The quenching of the spin–orbit splitting in the e vibrational levels is also a consequence of that distortion and will be discussed later. The very complex spectra that arise when the e vibronic levels of the $\tilde{A}^2A_1$ state are pumped differ so markedly from the symmetric mode spectra because, in this case, the optical transitions observed in fluorescence access a different set of ground-state levels. It is sufficient, for the present discussion, to note that the $\tilde{X}^2E$ vibrational levels can be characterized by a Jahn–Teller quantum number j where

$$j = \tfrac{1}{2}\Lambda + \sum_i l_i$$

Here, Λ can take values of +1 or −1 and the l_i are the usual vibrational angular momentum quantum numbers. Transitions

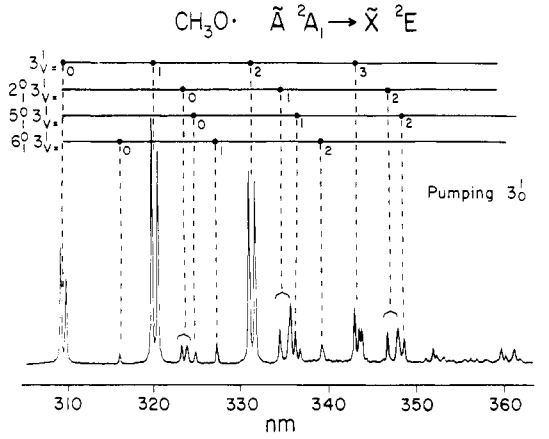

Figure 3. Laser-excited, wavelength-resolved emission spectrum of CH_3O using a monochromator and OMA. The assignments of the main peaks are indicated above the trace. The pump laser frequency coincides with the 3_0^1 excitation band. The OMA is gated open for 3.6 μs and delayed by 0.6 μs from the probe laser's firing. In this way scattered laser light is rejected and the emission lines near the laser pump frequency maintain their appropriate relative intensity with respect to the remainder of the spectrum. The monochromator slit width is 150 μm yielding an effective spectral resolution of $\approx$15 cm^{-1}. A total of 12000 laser pulses (10 min real time) was integrated to obtain the trace.

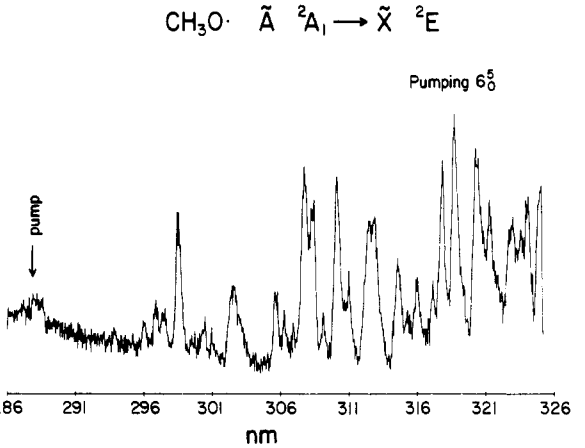

Figure 4. Laser-excited, wavelength-resolved emission spectrum of CH_3O. The pump frequency coincides with the band assigned as 6_0^5. The remaining experimental conditions are as in Figure 3, except the monochromator slit width has been widened to 500 μm and the integration time shortened to 8 min. No vibrational assignments have yet been made for this spectrum.

from the totally symmetric modes can only access the $j = {}^1/_2$ levels, whereas the e vibronic levels can emit to levels with higher values of j. A more detailed discussion can be found in a recent review article.[22]

The vibrational assignments made in this paper arise through a consideration of the single vibronic level (SVL) fluorescence spectra of only the totally symmetric modes. The present assignments are therefore for the $j = {}^1/_2$ levels of the ground state of methoxy. We defer to a subsequent publication a detailed analysis of the more complex degenerate-mode SVL spectra which contain information about the ground-state levels with $j \geq {}^3/_2$.

Just as in the excitation spectrum, the dominant feature of the fluorescence spectrum is expected to be ν_3'', the C–O stretching vibration. An examination of Figure 3 shows a strong series of doublets spaced by 1047 cm^{-1}. This interval is just the value expected for the C–O stretch (compare with the similar C–F stretching mode of CH_3F). The doubling represents the spin–orbit splitting of the ground state. Several other ν_3'' progressions are observed in Figure 3, starting 653, 1362 (doublet), and 1487 cm^{-1} from the center of the origin band. We assign the doublet feature at 1362 cm^{-1} to ν_2'', the totally symmetric umbrella mode of the molecule. The single lines are the Jahn–Teller active e vibrations ν_5'' and ν_6'', in which either the spin–orbital splitting has been

TABLE IV: CH_3O $\tilde{X}^2E$ Vibrational Intervals (in cm^{-1}) Observed in Dispersed Fluorescence

pumped bands								average interval		
0_0^0	3_0^1	3_0^2	3_0^3	3_0^4	3_0^5	2_0^1	$1_0^1 3_0^1$	rel to pump	spin–orbit splitting removed	assignt
0	0	0	0	0	0	0	0	0	0	origin
65	65	63	62	60	62	65	63	63		
683	687	687	684	678	682	685		685	653	ν_6
1047	1040	1048	1050	1041	1045	1050	1053	1047	1047	ν_3
1112	1108	1110	1114	1104	1109	1111	1109	1110		
			1234	1225	1232			1230	1198	$2\nu_6$
1371	1362	1348	1363	1349	1355	1369		1360	1362	ν_2
1424	1421	1431	1437	1428	1434	1422		1428		
1525	1516			1513	1520	1521		1519	1487	ν_5
			1644	1654	1657			1652	1620	$3\nu_6$
1747	1741	1746	1753	1737		1748		1745	1713	$\nu_3 + \nu_6$
					2049			2049	2017	$4\nu_6(?)$; $(\nu_2 + \nu_6)(?)$
2077	2068	2074	2081	2074		2075	2086	2076	2075	$2\nu_3$
2137	2132	2133	2140	2134		2135	2146	2137		
			2244	2237	2235			2239	2207	$\nu_3 + 2\nu_6$
				2287	2295			2291	2259	
2374	2367	2380	2392	2372	2371	2370		2375	2392	$\nu_2 + \nu_3$
2475	2469	2471	2478	2470	2467	2472		2472		
2524	2517		2527	2522	2521	2519		2522	2490	$\nu_3 + \nu_5$
2575	2566		2576	2568	2570			2571	2539	$\nu_2 + 2\nu_6$
			2667	2672	2684			2674	2642	$\nu_3 + 3\nu_6$
2793	2777	2784	2791			2778		2785	2753	$2\nu_3 + \nu_6$
				2800	2806		2812	2806[a]	2774	$\nu_4(?)$
				2852	2854			2853	2821	
							2937	2937[a]	2840[a]	ν_1
3091	3085	3086				3086		3087[b]		
3132	3126		3118	3110	3106			3118	3086	$\nu_2 + \nu_3 + \nu_6$
3156	3151	3149			3152	3151		3152[b]	3088	$3\nu_3$
3249			3266	3262	3257	3247		3256	3224	$2\nu_3 + 2\nu_6$
3397	3390	3398	3401	3397	3394	3392		3396	3413	$2\nu_3 + \nu_2$
3500	3493	3495		3486	3489	3494		3493		
							3523	3523	3491	$\nu_1 + \nu_6$
3554	3549		3554	3551	3549	3553		3552	3520	$2\nu_3 + \nu_5$

[a] Spin–orbit components of ν_1; $\nu_4(?)$ is blended with lowest frequency component. [b] Spin–orbit components of $3\nu_3$.

quenched to a value lower than our resolution (≈15 cm^{-1}) or, less likely, transition probability is only significant to one member of the spin–orbit split doublet.

Although the hydrogenic stretching modes ν_1'' and ν_4'' are not present in Figure 3, they have been observed when other excited-state vibrations are pumped and dispersed. The symmetric mode ν_1'', and its combinations with ν_3'', dominates the fluorescence spectrum when $1_0^1 3_0^1$ is pumped (Figure 5). The asymmetric mode ν_4'' has tentatively been assigned when 3_0^4 and 3_0^5 are pumped. A moderately strong feature is observed 2774 cm^{-1} from the pump wavenumber in both spectra. Although this interval is almost exactly equal to the $^2E_{3/2}$ component of ν_1'', the $^2E_{1/2}$ component is absent from 3_0^4 and is an order of magnitude weaker in 3_0^5. Further, the ratio of ν_1'/ν_1'' is 1.083, and, if this scaling factor is applied to ν_4', ν_4'' is predicted to be 2736 cm^{-1}. These facts suggest that the ν_4'' band may be accidentally degenerate with the $^2E_{3/2}$ component of ν_1''.

Table IV summarizes the various bands observed when the totally symmetric modes are pumped and dispersed together with their assignments. Table II again summarizes the observed fundamental vibrational frequencies. As expected, most of the fundamental vibrations occur in long progressions with ν_3''. It is also interesting to note that the overtones of ν_6'' are very prominent in some of the spectra, just as overtones of ν_6' were observed in excitation.

D. Spin–Orbit Splitting. The observed splitting of the ground vibrational state is 63 cm^{-1}, and this interval remains constant (to within our experimental error) in the ν_3'', $2\nu_3''$, and $3\nu_3''$ bands. The splitting observed in ν_2'' is 68 cm^{-1} but increases to 100 cm^{-1} in both $\nu_2'' + \nu_3''$ and $\nu_2'' + 2\nu_3''$. For ν_1'', $\nu_1'' + \nu_3''$, and $\nu_1'' + 2\nu_3''$, we observe a value of 131 cm^{-1}. As noted earlier, no splitting is resolved in any of the e vibrational modes. The fact that we see such large variations in the spin–orbit constant in the totally symmetric modes suggests to us that the Jahn–Teller effect must perturb these totally symmetric modes. This is unusual. Earlier

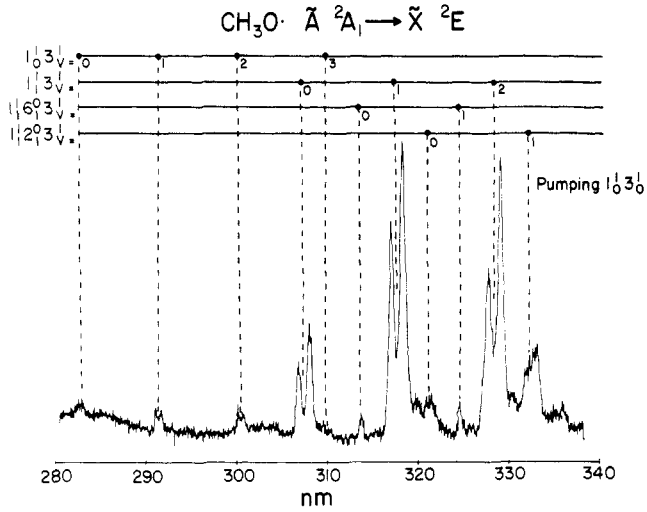

Figure 5. Laser-excited, wavelength-resolved emission spectrum of CH_3O observed when the band $1_0^1 3_0^1$ is pumped. The other experimental conditions are as in Figure 4.

studies[22] of the Jahn–Teller effect have employed models which only couple the Jahn–Teller active vibrations to the zero-point level. The present observations clearly demonstrate that a more complete model Hamiltonian is required to adequately fit the ground-state energy level pattern observed for CH_3O.

IV. Results: Perdeuteriomethoxy, CD_3O

A. Band Origin. The assignment of the 0_0^0 band of the CD_3O should be straightforward once the CH_3O molecule is assigned; only a small isotope shift is expected. However, the most prominent progression observed in the CD_3O excitation spectrum appears to start at 30924 cm^{-1} (the highest frequency band in Figure

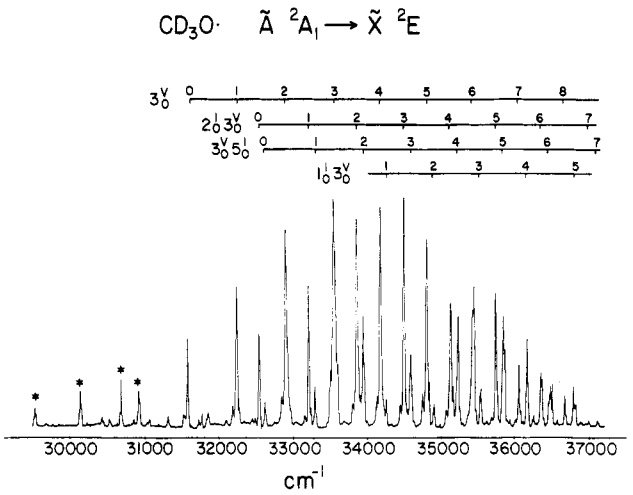

Figure 6. Laser excitation spectrum of CD_3O. The vibrational assignments are indicated above. The four relatively strong, low-frequency, bands marked with a * (and other weaker features in the same region) have very different rotational structure than the remaining bands in the spectrum. It is therefore believed that they arise either from highly excited vibrational levels of CD_3O or from another molecular species. See the text for details.

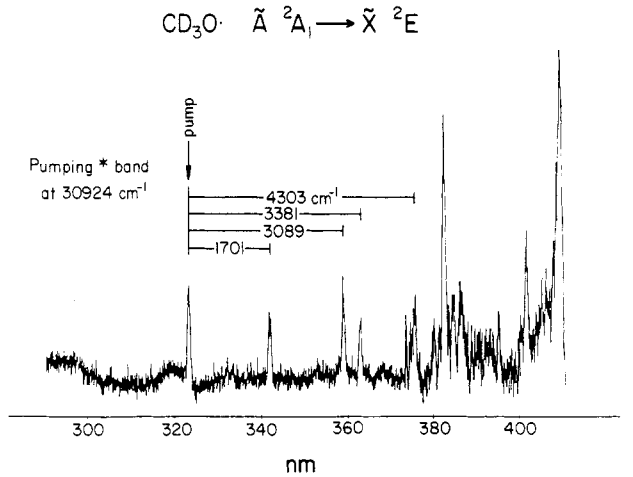

Figure 7. Laser-excited, wavelength-resolved emission spectrum of CD_3O observed when the 30924 "starred" band of Figure 6 is excited. Other conditions are the same as in Figure 3, except the monochromator slit width is 1 mm.

6 marked with a *) with a regular ~660-cm^{-1} vibrational spacing. This vibrational interval is the expected C–O stretch which shows little change from CH_3O. However, the assignment of the 30924-cm^{-1} band as the electronic origin would imply that the deuteration has caused a 700-cm^{-1} isotope shift. This is very improbable. The possibility that the CH_3O spectrum is misassigned has been ruled out by a careful search for, and nonobservation of, another member of the C–O stretching vibration to the red of the CH_3O 0_0^0 band. A closer examination of the CD_3O excitation spectrum suggests that the starred band does not belong to the ν_3' progression[26] and that the true $\tilde{A}^2A_1 \rightarrow \tilde{X}^2E_{3/2}$ origin value is the next band in the progression at 31581 cm^{-1}. (Given that the ground-state spin–orbit splitting is 54 cm^{-1} in CD_3O, the traditional, mean origin value is reduced to 31554 cm^{-1}.) This implies a much smaller, and more reasonable, isotope shift of 64 cm^{-1}.

Several pieces of evidence lead to this conclusion. First, the rotational structure of all the starred bands differs considerably from the remaining members of the ν_3' progression, suggesting either a different vibronic symmetry or different species. Second,

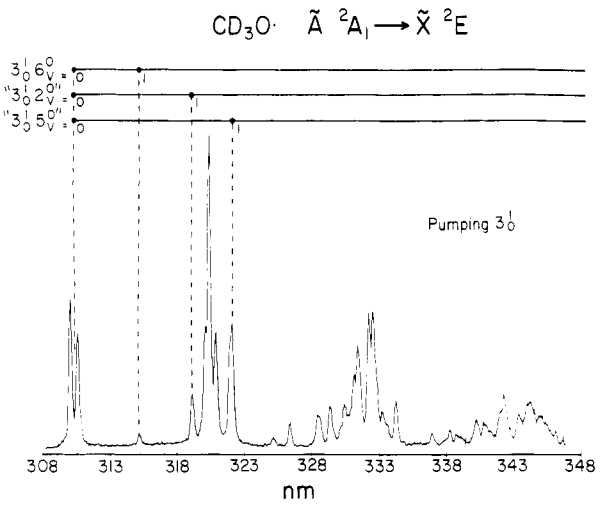

Figure 8. Laser-excited, wavelength-resolved emission spectrum of CD_3O observed when the 3_0^1 band is excited. Other conditions are the same as Figure 3. Quotation marks indicate that assignments are tentative.

when emission from the 30924-cm^{-1} starred band is dispersed, the majority of the fluorescence is emitted far to the red of the pump line (Figure 7). This is quite different from the other members of the progression (see, for example, Figure 8). (An unfortunate consequence of this red-shifted fluorescence is that the signal-to-noise ratio in the region of the pump laser's wavelength is poor, and we cannot definitively say whether the feature is hot. That is, we cannot convincingly observe any features to the blue of our pump laser.) A third piece of evidence is that the dispersed fluorescence spectrum of the starred band, Figure 7, shows a single peak at the pump wavelength rather than the spin–orbit doublet which arises when the ground electronic state vibrationless level is pumped.

These characteristic features of the 30924-cm^{-1} band are also seen in the other three strong starred excitation features that lie to the red of the assigned origin band in Figure 6. It is interesting that Brossard et al.[10] also observed these four bands in their emission study of CD_3O from a different precursor. (A constant 20-cm^{-1} difference in wavenumber between this study and that of ref 10 can be explained by a different rotational temperature and, hence, different envelope maxima.) We cannot rule out the possibility that these bands are due to an impurity, but it seems more likely that they are unidentified CD_3O hot bands, with the resulting conclusion that CD_3O is vibrationally hotter in our experiment than CH_3O.

B. Vibrational Assignment of the $\tilde{A}^2A_1$ State. The wavenumbers of the bands observed in excitation are listed in Table V. Most of the bands lie in a series of progressions with a ~660-cm^{-1} vibrational spacing. This interval corresponds to ν_3', and the 663-cm^{-1} separation between 0_0^0 and 3_0^1 is numerically almost identical with ν_3' for CH_3O. Three additional progressions are seen in the spectrum starting 971, 1047, and 2678 cm^{-1} to the blue of the origin. The two lower frequency vibrations are ν_2' and ν_5', but it is not immediately clear which is which. An inspection of the rotational structure of the 971- and 1047-cm^{-1} bands clearly identifies them as having a_1 and e vibronic symmetry, respectively. Thus, we assign ν_2' as 971 cm^{-1} and ν_5' as 1047 cm^{-1}. The remaining frequency, 2678 cm^{-1}, is too large for a C–D stretching motion and must include 1 quantum of C–O stretch. We assign the 2678-cm^{-1} band as $1_0^1 3_0^1$. This choice was made, rather than $3_0^1 4_0^1$, because the rotational structure is very similar to the origin and because in CH_3O ν_1' only appears in combination with ν_3', whereas 4_0^1 itself was observed. Thus ν_1' = 2015 cm^{-1}. These excited-state vibrational frequencies are listed in Table VI, where the vibrational frequencies of the similar CD_3F and CD_3Cl molecules are listed.

(26) The umbrella motion of CD_3O will lie at a lower frequency than the C–O stretch and hence, by convention, the ν_2 and ν_3 labels should be exchanged. However, we feel that it is less confusion to continue to label the C–O stretch as ν_3 and the umbrella as ν_2.

(27) Jones, E. W.; Popplewell, R. J. L.; Thompson, H. W. *Proc. R. Soc. London, A* **1966**, *290*, 490.
(28) Caldow, G. L.; Duxbury, G. *J. Mol. Spectrosc.* **1981**, *89*, 93.

TABLE V: CD_3O $\tilde{A}^2A_1 \leftarrow \tilde{X}^2E$ Excitation Spectrum (cm^{-1})

wave-number[a]	rel wavenumber[a]	assignt	wave-number[a]	rel wavenumber[a]	assignt
29542	−2039	*	33945	2364	$3_0^2 5_0^1$
30150	−1431	*	34179	2598	3_0^4
30449	−1132		34259	2678	$1_0^1 3_0^1$
30551	−1030		34495	2914	$2_0^1 3_0^3$
30704	−877	*	34586	3005	$3_0^3 5_0^1$
30924	−657	*	34801	3220	3_0^5
31027	−554		34902	3321	$1_0^1 3_0^2$
31060	−521	6_1^0	35147	3566	$2_0^1 3_0^4$
31309	−272		35224	3643	$3_0^5 5_0^1$
31581	0	0_0^0	35431	3850	3_0^6
31728	147		35538	3957	$1_0^1 3_0^3$
31773	192		35744	4163	$2_0^1 3_0^5$
31857	276		35854	4273	$3_0^5 5_0^1$
32103	522		36060	4479	3_0^7
32244	663	3_0^1	36171	4590	$1_0^1 3_0^4$
32552	971	2_0^1	36361	4780	$2_0^1 3_0^6$
32628	1047	5_0^1	36486	4905	$3_0^6 5_0^1$
32900	1319	3_0^2	36672	5091	3_0^8
33210	1629	$2_0^1 3_0^1$	36797	5216	$1_0^1 3_0^5$
33292	1711	$3_0^1 5_0^1$	36988	5407	$2_0^1 3_0^7$
33554	1973	3_0^3	37108	5527	$3_0^7 5_0^1$
33859	2278	$2_0^1 3_0^2$			

[a] Companion peaks at 50 cm^{-1} to lower frequency are observed for the strong peaks but are not indicated in the table. Presumably these transitions arise from the $^2E_{1/2}$ state.

TABLE VI: Observed Vibrational Fundamentals (in cm^{-1}) for Several CD_3X Symmetric Tops

	$\tilde{X}$ CD_3F[a]	$\tilde{X}$ CD_3Cl[b]	$\tilde{X}$ CD_3O	$\tilde{A}$ CD_3O
ν_1	2091	2161		2015
ν_2	1135	1029	893(?)	971
ν_3	992	695	1012(?)	663
ν_4	2259	2286		
ν_5	1072[c]	1058	1174	1047
ν_6	912	775	496	

[a] Reference 27. [b] Reference 23. [c] Reference 28.

C. Vibrational Assignment of the $\tilde{X}^2E_i$ State. The 3_0^1 dispersed fluorescence spectrum shown in Figure 8 is typical of the CD_3O spectra and demonstrates some of the problems found when the ground-state vibrational structure is assigned. On deuteriation, the ν_2'', ν_3'', ν_5'', and $2\nu_6''$ vibrations are all expected to lie close to 1000 cm^{-1}. An even more complex picture is expected near 2000 cm^{-1}, where ν_1'', $2\nu_2''$, $2\nu_3''$, ν_4'', $2\nu_5''$, and $4\nu_6''$ are clustered. This leads to the characteristic "clumped" spectrum shown in Figure 8, and assignments become difficult to make. Table VII lists the ground-state intervals observed when the indicated modes of the $\tilde{A}^2A_1$ state are pumped. The lowest frequency vibration, 496 cm^{-1}, is assigned as ν_6''. It lies close to the value estimated by assuming a $2^{1/2}$ isotopic dependence.

A second vibrational interval, 1174 cm^{-1}, can be assigned with some confidence as ν_5''. This vibrational frequency is too small for ν_4'' or ν_1'', and ν_2'' is expected to lie at lower frequency than ν_5''. The fact that the 1174-cm^{-1} vibration is enhanced when $5_0^1 3_0^4$ is pumped further supports this assignment.

It is difficult to assign any of the other ground-state vibrational frequencies with confidence, and the following discussion must be regarded as speculative. Figure 9, which shows the 2_0^1 dispersed fluorescence spectrum, is quite simple. When compared with the 3_0^1 spectrum (Figure 8), the 893-cm^{-1} band is seen to have gained considerable intensity, perhaps suggesting that it is ν_2''. A study of the other spectra listed in Table VII shows that a consistent picture can only be obtained if this is the only component of ν_2''. That is, the spin–orbit splitting in ν_2'' must have been quenched below our experimental resolution (or only one component has appreciable oscillator strength). This ν_2'' value is smaller than expected, on the basis of simple isotope relationships, but ν_2'' will almost certainly be perturbed to lower frequency by Fermi resonance with ν_3''.

When the members of the ν_3' progression are pumped, the 1012-cm^{-1} band is prominent; again, the spin–orbit splitting must be small to form a consistent picture if this band is assigned as ν_3''. It might also be noted that the 967- and 1033-cm^{-1} bands appear to form a strong spin–orbit doublet which appears when

TABLE VII: CD_3O $\tilde{X}^2E$ Vibrational Intervals (in cm^{-1}) Observed in Dispersed Fluorescence

pumped bands							average interval		
0_0^0	3_0^1	3_0^2	2_0^1	$2_0^1 3_0^4$	$1_0^1 3_0^3$	$5_0^1 3_0^4$	rel to pump	spin–orbit splitting removed	assignt
0	0	0	0	0	0	0	0	0	origin
56	54	55	57	54	51	52	54		
516	517	523		520	534	530	523	496	ν_6
				722	742	739	734	707	
915	918	923	920	922	921	919	920	893	ν_2(?)
948[a]							948	921	
					993	995	994	967	
				1015[a]			1015	988	
1036	1039	1048	1029	1045			1039	1012	ν_3(?)
					1063	1056	1060	1033	
1083	1086	1093					1087	1060	
1196	1198	1205	1201	1202	1205	1201	1201	1174	ν_5
				1287		1284	1286	1259	
1487	1486	1499		1496	1502	1487	1493	1466	
1609	1606	1617				1625	1614	1587	
				1708	1723		1716	1689	
1804	1808	1815	1819	1807		1820	1812	1785	
1886	1889	1900	1904	1913	1907	1897	1899	1872	
1986	1990	1976	1995		2001	1989	1990	1963	
			2026	2012	2024	2036	2025	1998	
2054	2067				2051		2057	2030	
		2087		2093		2101	2094	2067	
2146	2151	2159		2157			2153	2126	
2170	2175	2189	2183	2188			2181	2154	
		2210			2195	2204	2203	2176	
				2249	2266		2257	2230	
2326	2331	2334		2341	2343		2335	2308	
					2460		2460	2433	
2565	2570			2578	2584		2574	2547	
2680	2683	2687		2692	2678	2663	2681	2654	
2723	2730		2732				2728	2701	

[a] Shoulder.

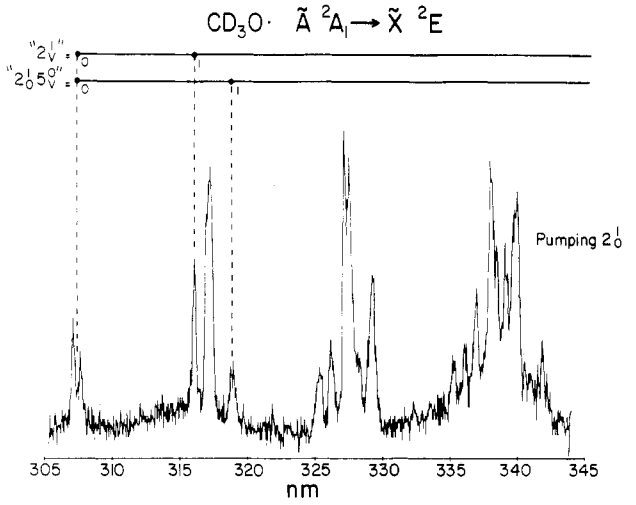

Figure 9. Laser-excited, wavelength-resolved emission spectrum of CD_3O observed when the 2_0^1 band is excited. Other conditions are the same as Figure 3, except the slit width is 200 μm. Quotation marks indicate that assignments are tentative.

$1_0^1 3_0^4$ and $5_0^1 3_0^4$ are pumped. The center of the doublet is 1000 cm^{-1} from the origin, but it is not obvious how this band should be assigned. The CO stretch is a candidate, but this doublet is not present in the 0_0^0 or 3_0^x spectra.

A fundamental problem exists when attempting to assign these spectra. There are simply too many discrete features in the region below 1200 cm^{-1}. Table VII lists 10 intervals; the number might be reduced to 8 if the 921-cm^{-1} shoulder is considered to be a blend of the 893- and 967-cm^{-1} lines and if the 988-cm^{-1} feature is considered a blend of the 1012- and 967-cm^{-1} bands. However, even this reduced number cannot be explained in terms of a simple vibrational picture. As noted above, the ν_6'' and ν_5'' vibrations are singlets, just as in CH_3O. This leaves six features to be accounted for by ν_2'', ν_3'', and $2\nu_6''$. By analogy with CH_3O, the latter vibration is almost certainly a singlet at our resolution, and ν_2'' and ν_3'' also do not appear to be doubled. The 707-cm^{-1} vibration is particularly difficult to explain. It is too small for ν_2'' or ν_3'', and if it is $2\nu_6''$, this vibration is extremely anharmonic. One possible explanation for the large number of bands is that the dispersed fluorescence spectra show transitions to levels other than the $j = {}^1/_2$ set normally allowed from the totally symmetric levels of the $\tilde{A}^2A_1$ state. Some evidence in favor of this explanation is provided when the $5_0^1 3_0^4$ pumped fluorescence is compared to the other totally symmetric modes. All of the ground-state intervals observed when this e vibronic level of the Ã state is pumped are observed from the totally symmetric pumped levels. This is in stark contrast to the CH_3O spectra discussed earlier and is very surprising.

It is clear that a complete Jahn–Teller analysis will be required to unravel the details of the vibrational structure of $\tilde{X}^2E$ CD_3O.

V. Conclusions

A relatively complete picture of the vibronic structure of CH_3O has been provided by its jet-cooled excitation spectrum and its laser-excited, wavelength-resolved emission spectrum. A new value for the origin of the $\tilde{A}^2A_1 \leftrightarrow \tilde{X}^2E$ electronic transition has been obtained, which should be of significance to both spectroscopic and dynamical work involving methoxy. An essentially complete set of vibrational frequencies has been obtained for both the Ã and $\tilde{X}$ states of CH_3O.

Similar investigations of CD_3O have yielded consistent, but considerably less illuminating results. The excitation spectrum shows most of the corresponding features that were observed for CH_3O. However, several unassigned bands, of quite different structure, are also observed near the origin. The wavelength-resolved emission spectrum of CD_3O is complicated by several factors involving the clustering of the $n\nu_1''$, $2n\nu_2''$, $2n\nu_3''$, $n\nu_4''$, $2n\nu_5''$, and $4n\nu_6''$ transitions. Significant interactions among several (or all) of these levels make precise spectral analysis exceedingly difficult.

Acknowledgment. This work was supported by the National Science Foundation under Grant CHE-8507537.

Registry No. MeO, 2143-68-2; O_2, 7782-39-0.

Single-Pulse Raman Scattering Study of Triaminotrinitrobenzene under Shock Compression

Wayne M. Trott* and Anita M. Renlund

Sandia National Laboratories, Albuquerque, New Mexico 87185 *(Received: February 9, 1988)*

Pulsed-laser-excited Raman scattering methods have been used to examine the dynamic molecular-level response of an explosive molecule (triaminotrinitrobenzene, TATB) to sustained shock loading at a fused silica window interface. The anomalous behavior of Raman modes associated with nitro groups in the molecule (the 881-cm^{-1} NO_2 deformation mode, the 1146-cm^{-1} symmetric C–NO_2 stretching mode, and the 1170-cm^{-1} totally symmetric NO_2 stretching mode) is compared to results obtained under static high pressure. The shock compression data indicate that elevated temperatures act to restrain pressure-enhanced coupling of NO_2 and NH_2 groups in the molecule. Differences in the spectra obtained under static and dynamic high-pressure conditions are discussed in relation to the known insensitivity of TATB to shock initiation.

Introduction

There is growing interest in the development and use of new experimental techniques to study the time-dependent, molecular-level response of condensed-phase materials to the extreme pressure, density, and temperature conditions achieved during shock compression.[1] In the area of fundamental explosives research, this interest is motivated by the desire to acquire insight into the relevant physical and chemical processes leading to initiation and sustained detonation. Various optical methods have been used to probe shocked and detonating energetic materials, including emission and absorption spectroscopy as well as spontaneous and nonlinear Raman scattering techniques.[2] Much of

(1) Duvall, G. E. In *Proceedings of the Fourth American Physical Society Topical Conference on Shock Waves in Condensed Matter*, Gupta, Y. M., Ed.; Plenum: New York, 1986; p 1.

(2) Schmidt, S. C.; Moore, D. S.; Shaner, J. W. *Diagnostics for Determining Phenomenology of Condensed-Phase Shock-Compressed Molecular Systems*; Los Alamos National Laboratory Report; LA-UR 83-901, March, 1983.

0022-3654/88/2092-5921$01.50/0 © 1988 American Chemical Society